Azido Derivatives of Low-Valent Group 14 Elements: Synthesis, Characterization, and Electronic Structure of [(*n*-Pr)$_2$ATI]GeN$_3$ and [(*n*-Pr)$_2$ATI]SnN$_3$ Featuring Heterobicyclic 10-π-Electron Ring Systems

Ashley E. Ayers, Dennis S. Marynick,* and H. V. Rasika Dias*

Department of Chemistry and Biochemistry, The University of Texas at Arlington, Arlington, Texas 76019-0065

Received May 23, 2000

Treatment of THF solutions of [(*n*-Pr)$_2$ATI]MCl (where [(*n*-Pr)$_2$ATI]$^-$ = *N*-(*n*-propyl)-2-(*n*-propylamino)-troponiminate; M = Ge and Sn) with sodium azide affords the compounds [(*n*-Pr)$_2$ATI]MN$_3$ in excellent yield. X-ray analyses revealed that these Ge(II) and Sn(II) compounds feature linear azide moieties and planar heterobicyclic C$_7$N$_2$M ring systems. Germanium and tin atoms adopt a pyramidal geometry. IR spectra of [(*n*-Pr)$_2$ATI]GeN$_3$ and [(*n*-Pr)$_2$ATI]SnN$_3$ display a $\nu_{asym}(N_3)$ band at 2048 and 2039 cm^{-1}, respectively. DFT calculations on the corresponding methyl-substituted species demonstrate that the geometrical and electronic structure of these two species are very similar, and the dominant canonical form of the metal−azide moiety is M−N−N≡N. The tin system is, as expected, slightly more ionic. A comparative CASSCF/DFT study on the model system H−Sn−N$_3$ illustrates that the DFT approach is viable for the calculation of the structures of these species.

Introduction

Metal and nonmetal species containing the azide functionality have been known for many years.[1−5] These compounds are of interest as starting materials for various organic and inorganic compounds,[2,3,6−9] as explosives,[3,4,10−12] and as new magnetic materials.[13−16] Azido derivatives of carbon represent the most widely studied group among the azides.[2,3] Related azides of heavier group 14 members such as those of silicon(IV) and tin-(IV) are also fairly well-known.[4,5,17] In contrast, very little is known about the azides of low-valent group 14 elements.[17] The germanium(II) adduct [HB(3,5-(CH$_3$)$_2$Pz)$_3$]GeN$_3$ and the lead-(II) species Pb(N$_3$)$_2$ are the only well-characterized compounds of this type in the literature to our knowledge.[17−19]

An area of research focus in this laboratory is the chemistry of *N*-alkyl-2-(alkylamino)troponiminate ([(R)$_2$ATI]$^-$) derivatives of main group elements.[20−26] This ligand [(R)$_2$ATI]$^-$, which features a delocalized 10-π-electron ligand backbone, has not been used widely in main group chemistry.[20] Recently, we reported the use of the diisopropyl version of this ligand to stabilize cationic Ge(II) and Sn(II) species, e.g., {[(*i*-Pr)$_2$ATI]Ge}$^+$ and {[(*i*-Pr)$_2$ATI]Sn}$^+$.[22,25] In this paper, we describe use of the *N*-(*n*-propyl)-2-(*n*-propylamino)troponiminate ligand ([(*n*-Pr)$_2$ATI]$^-$) to isolate azido derivatives of germanium(II) and tin(II), and we present theoretical calculations which demonstrate that these two systems are very similar both electronically and structurally.

General Procedures. All manipulations were carried out under an atmosphere of purified nitrogen either using standard Schlenk techniques or in a Vacuum Atmospheres single-station drybox equipped with a −25 °C refrigerator. Solvents were purchased from commercial sources and distilled from conventional drying agents prior to use. Glassware was oven-dried at 150 °C overnight. The NMR spectra were recorded at room temperature on a JEOL Eclipse 500 spectrometer (^{1}H, 500.16 MHz; ^{13}C, 125.78 MHz). Proton and carbon chemical shifts are reported in parts per million vs Me$_4$Si. Infrared spectra were recorded on a JASCO FT-IR 410 spectrometer. Melting points were obtained on a Mel-Temp II apparatus. Elemental analyses

(1) *Chemistry of Pseudohalides*; Golub, A. M., Kohler, H., Skopenko, V. V., Eds.; Elsevier: New York, 1986; p 28.
(2) *The Chemistry of the Azido Group*; Patai, S., Ed.; Interscience: New York, 1971.
(3) *Azides and Nitrenes: Reactivity and Utility*; Scriven, E. F. V., Ed.; Academic: New York, 1984.
(4) Tornieporth-Oetting, I. C.; Klapötke, T. M. *Angew. Chem., Int. Ed. Engl.* **1995**, *34*, 511.
(5) Thayer, J. S. *Organomet. Chem. Rev.* **1966**, *1*, 157.
(6) Lwowski, W. *Nitrenes*; Interscience: New York, 1970.
(7) Nugent, W. A.; Mayer, J. M. *Metal-Ligand Multiple Bonds*; John Wiley & Sons: New York, 1988.
(8) Nugent, W. A.; Haymore, B. L. *Coord. Chem. Rev.* **1980**, *31*, 123.
(9) Wigley, D. E. *Prog. Inorg. Chem.* **1994**, *42*, 239.
(10) Klapötke, T. M. *Chem. Ber.* **1997**, *130*, 443.
(11) *Kirk-Othmer Encyclopedia of Chemical Technology*, 2nd ed.; 1965; Vol. 8, p 584.
(12) *Kirk-Othmer Encyclopedia of Chemical Technology*, 3rd ed.; 1980; Vol. 9, p 570.
(13) Monfort, M.; Resino, I.; Ribas, J.; Stoeckli-Evens, H. *Angew. Chem., Int. Ed.* **2000**, *39*, 191.
(14) Ribas, J.; Monfort, M.; Resino, I.; Solans, X.; Rabu, P.; Maingot, F.; Drillon, M. *Angew. Chem., Int. Ed. Engl.* **1996**, *35*, 2520.
(15) Escuer, A.; Vicente, R.; Goher, M. A. S.; Mautner, F. A. *Inorg. Chem.* **1998**, *37*, 782.
(16) Cortes, R.; Lezama, L.; Mautner, F. A.; Rojo, T. In *Molecular-Based Materials: Theory, Techniques, and Applications*; Turnbull, M. M., Sugimoto, T., Thompson, L. K., Eds.; American Chemical Society: Washington, DC, 1996; p 187.
(17) Filippou, A. C.; Portius, P.; Kociok-Köhn, G. *Chem. Commun.* **1998**, 2327 and references therein.
(18) *The Merck Index*, 11th ed.; Budavari, S., Ed.; Merck & Co., Inc.: Rahway, NJ, 1989; p 5274 and references therein.
(19) Choi, C. S.; Prince, E.; Garrett, W. L. *Acta Crystallogr.* **1977**, *B33*, 3536.
(20) Dias, H. V. R.; Wang, Z.; Jin, W. *Coord. Chem. Rev.* **1998**, *176*, 67.
(21) Dias, H. V. R.; Jin, W.; Ratcliff, R. E. *Inorg. Chem.* **1995**, *34*, 6100.
(22) Dias, H. V. R.; Jin, W. *J. Am. Chem. Soc.* **1996**, *118*, 9123.
(23) Dias, H. V. R.; Jin, W. *Inorg. Chem.* **1996**, *35*, 6546.
(24) Dias, H. V. R.; Jin, W.; Wang, Z. *Inorg. Chem.* **1996**, *35*, 6074.
(25) Dias, H. V. R.; Wang, Z. *J. Am. Chem. Soc.* **1997**, *119*, 4650.
(26) Dias, H. V. R.; Jin, W. *J. Chem. Crystallogr.* **1997**, *27*, 353.

10.1021/ic000545u CCC: $19.00
Published on Web 08/17/2000

were performed at the University of Texas at Arlington using a Perkin-Elmer model 2400 CHN analyzer. [(*n*-Pr)$_2$ATI]GeCl and [(*n*-Pr)$_2$ATI]SnCl were prepared using a procedure similar to that described for the *N*-isopropyl analogues.[22,25]

[(*n*-Pr)$_2$ATI]GeN$_3$. [(*n*-Pr)$_2$ATI]GeCl (150 mg, 0.48 mmol) and NaN_3 (31 mg, 0.48 mmol) were mixed in THF (10 mL) at room temperature. The solution turned a bright orange color. After the solution was stirred overnight, the THF was removed under vacuum. The remaining solid was extracted into toluene and filtered through Celite. Removal of toluene under vacuum gave a yellow-orange solid (140 mg, 92%). X-ray quality crystals were grown from hexane at room temperature. Mp.: 56−58 °C (the sample decomposes to a red oily liquid). ^{1}H NMR ($CDCl_3$): δ 1.06 (t, 6H, J = 7.5 Hz, CH_3CH$_2$CH$_2$), 1.91 (m, 4H, CH$_3$CH_2CH$_2$), 3.62 (m, 4H, CH$_3$CH$_2$CH_2), 6.69 (t, 1H, J = 9.4 Hz, H$_5$), 6.77 (d, 2H, J = 11.3 Hz, H$_{3,7}$), 7.27 (m, 2H, H$_{4,6}$). ^{13}C{^{1}H} NMR ($CDCl_3$): δ 12.0 (*C*H$_3$CH$_2$CH$_2$), 22.2 (CH$_3$*C*H$_2$CH$_2$), 48.4 (CH$_3$CH$_2$*C*H$_2$), 114.7 (C$_5$), 122.7 (C$_{3,7}$), 137.1 (C$_{4,6}$), 160.8 (C$_{2,8}$). IR (KBr, cm^{-1}): 3290, 2952, 2924, 2859, 2048 (asym N$_3$), 1591, 1513, 1438, 1418, 1393, 1378, 1351, 1276, 1234, 1082, 1001, 882, 739, 570. IR (in toluene, cm^{-1}): 2056 (asym N$_3$). Anal. Calcd for $C_{13}H_{19}N_5Ge$: C, 49.11; H, 6.02; N, 22.03. Found: C, 48.85; H, 5.78; N, 21.51.

[(*n*-Pr)$_2$ATI]SnN$_3$. [(*n*-Pr)$_2$ATI]SnCl (200 mg, 0.56 mmol) and NaN_3 (37 mg, 0.57 mmol) were mixed in THF (10 mL) at room temperature. The solution turned a bright orange color. After the solution was stirred overnight, the THF was removed under vacuum. The remaining solid was extracted into toluene and filtered through Celite. Removal of toluene under vacuum gave a yellow-orange solid (190 mg, 93%). X-ray quality crystals were grown from toluene−hexane at room temperature. Mp: 93−94 °C. ^{1}H NMR ($CDCl_3$): δ 1.09 (t, 6H, J = 7.2 Hz, CH_3CH$_2$CH$_2$), 2.00 (m, 4H, CH$_3$CH_2CH$_2$), 3.60 (m, 4H, CH$_3$CH$_2$CH_2), 6.61 (t, 1H, J = 9.3 Hz, H$_5$), 6.73 (d, 2H, J = 11.5 Hz, H$_{3,7}$), 7.24 (m, 2H, H$_{4,6}$). ^{13}C{^{1}H} NMR ($CDCl_3$): δ 12.2 (*C*H$_3$CH$_2$CH$_2$), 24.1 (CH$_3$*C*H$_2$CH$_2$), 50.7 (CH$_3$CH$_2$*C*H$_2$), 115.2 (C$_5$), 121.7 (C$_{3,7}$), 136.1 (C$_{4,6}$), 163.2 (C$_{2,8}$). IR (KBr, cm^{-1}): 3329, 2959, 2922, 2870, 2039 (asym N$_3$), 1590, 1508, 1437, 1414, 1390, 1366, 1308, 1270, 1229, 1069, 996, 885, 727, 553, 537. IR (in toluene, cm^{-1}): 2051 (asym N$_3$). Anal. Calcd for $C_{13}H_{19}N_5Sn$: C, 42.89; H, 5.26; N, 19.24. Found: C, 42.46; H, 5.03; N, 18.98.

X-ray Structure Determination. A suitable crystal covered with a layer of hydrocarbon oil was selected, attached to a glass fiber, and immediately placed in the low-temperature nitrogen stream. Data collections were carried out at low temperature on a Siemens P4 diffractometer equipped with an LT-2A device for low-temperature work and graphite-monochromated Mo Kα radiation (λ = 0.71073 Å). The unit cell parameters of [(*n*-Pr)$_2$ATI]GeN$_3$ and [(*n*-Pr)$_2$ATI]SnN$_3$ were determined by least-squares refinement of 39 reflections. Three standard reflections were measured at every 97 data points to check for crystal deterioration and/or misalignment. No significant deterioration in intensity was observed. Data were corrected for Lorentz, polarization, and absorption (using ψ scans) effects. Structures were solved by direct methods followed by successive cycles of full-matrix least-squares refinement on F^2 and difference Fourier analysis. All the non-hydrogen atoms were refined anisotropically. The hydrogen atoms were included at calculated positions. They were treated as riding atoms with isotropic displacement parameters fixed 1.2 or 1.5 times the value refined for the respective host atom. Software programs and the sources of scattering factors are contained in the Bruker SHELXTL 5.1 software package provided by the Bruker Analytical X-ray Instruments, Inc. Some details of data collection and refinements are given in Table 1. Bond distances and angles are given in Tables 2 and 3.

Table 1. Crystal Data and Summary of Data Collection and Refinement

	[(*n*-Pr)$_2$ATI]GeN$_3$	[(*n*-Pr)$_2$ATI]SnN$_3$
formula	$C_{13}H_{19}GeN_5$	$C_{13}H_{19}SnN_5$
fw	317.92	364.02
space group	P$\bar{1}$	P$\bar{1}$
T, K	198(2)	198(2)
λ, Å	0.71073	0.71073
a, Å	7.5389(10)	7.9221(10)
b, Å	9.5627(16)	10.1385(13)
c, Å	11.0499(17)	19.989(3)
α, deg	94.848(13)	90.465(14)
β, deg	109.876(10)	91.358(12)
γ, deg	100.905(12)	111.820(9)
V, Å^3	726.01(19)	1489.8(4)
Z	2	4
ρ(calc), g/cm^3	1.454	1.623
μ, mm^{-1}	2.104	1.710
R1, wR2 [$I > 2\sigma(I)$][a]	0.0211, 0.0527	0.0253, 0.0667
R1, wR2 (all data)[a]	0.0216, 0.0530	0.0279, 0.0683

[a] R1 = $\sum||F_o| - |F_c||/\sum|F_o|$ and wR2 = $[\sum[w(F_o^2 - F_c^2)^2]/\sum[w(F_o^2)^2]]^{1/2}$.

Table 2. Bond Lengths (Å) and Angles (deg) for [(*n*-Pr)$_2$ATI]GeN$_3$

Ge−N(1)	1.945(2)	C(2)−C(8)	1.474(3)
Ge−N(9)	1.956(2)	C(3)−C(4)	1.378(4)
Ge−N(2)	2.047(2)	C(4)−C(5)	1.384(4)
N(1)−C(2)	1.332(3)	C(5)−C(6)	1.381(4)
N(1)−C(10)	1.466(3)	C(6)−C(7)	1.378(4)
N(2)−N(3)	1.197(3)	C(7)−C(8)	1.407(4)
N(3)−N(4)	1.144(4)	C(10)−C(11)	1.522(3)
N(9)−C(8)	1.336(3)	C(11)−C(12)	1.522(3)
N(9)−C(13)	1.472(3)	C(13)−C(14)	1.510(4)
C(2)−C(3)	1.407(3)	C(14)−C(15)	1.522(3)
N(1)−Ge−N(9)	79.68(8)	C(3)−C(2)−C(8)	125.3(2)
N(1)−Ge−N(2)	96.92(9)	C(4)−C(3)−C(2)	131.6(2)
N(9)−Ge−N(2)	95.87(9)	C(3)−C(4)−C(5)	130.2(2)
C(2)−N(1)−C(10)	122.7(2)	C(6)−C(5)−C(4)	125.6(3)
C(2)−N(1)−Ge	117.9(1)	C(7)−C(6)−C(5)	130.9(3)
C(10)−N(1)−Ge	119.3(2)	C(6)−C(7)−C(8)	131.3(2)
N(3)−N(2)−Ge	115.3(2)	N(9)−C(8)−C(7)	122.1(2)
N(4)−N(3)−N(2)	177.5(3)	N(9)−C(8)−C(2)	112.9(2)
C(8)−N(9)−C(13)	120.4(2)	C(7)−C(8)−C(2)	125.1(2)
C(8)−N(9)−Ge	117.1(1)	N(1)−C(10)−C(11)	113.0(2)
C(13)−N(9)−Ge	122.4(1)	C(10)−C(11)−C(12)	111.5(2)
N(1)−C(2)−C(3)	122.4(2)	N(9)−C(13)−C(14)	113.0(2)
N(1)−C(2)−C(8)	112.3(2)	C(13)−C(14)−C(15)	110.1(2)

Computational Procedures

Geometries of both species (with methyl groups substituted for the *n*-Pr substituents) were fully optimized with Gaussian 98[27] at the B3LYP[28] level using a basis set denoted as **B1**. C_s symmetry was assumed. The **B1** basis set was constructed as follows: for C and H, 6-31G*, for N, 6-31+G*; and for Ge-(Sn), the Stuttgart−Dresden (SDD) relativistic ECP basis set[29] supplemented with d type polarization functions (ζ = 0.264 for Ge and 0.183 for Sn). A natural bond orbital analysis[30] was performed for each species at the optimized geometry, which was also characterized by a force constant/frequency calculation. A second conformation of each species, in which the azide ligand is trans to the [(Me)$_2$ATI]$^-$ ligand, was also optimized.

To test the accuracy of the DFT approach for the calculation of the molecular geometries of these species, a CASSCF geometry optimization was carried out on a much smaller model system, H−Sn−N$_3$, using the program GAMESS.[31] This

Table 3. Bond Lengths (Å) and Angles (deg) for $[(n\text{-Pr})_2\text{ATI}]SnN_3$

Sn(1)−N(9)	2.156(3)	N(9)−C(13)	1.467(5)
Sn(1)−N(1)	2.190(3)	N(16)−C(17)	1.331(5)
Sn(1)−N(2)	2.253(4)	N(16)−C(25)	1.473(5)
Sn(2)−N(24)	2.166(3)	N(24)−C(23)	1.336(5)
Sn(2)−N(16)	2.173(3)	N(24)−C(28)	1.460(5)
Sn(2)−N(2′)	2.230(5)	C(2)−C(3)	1.419(5)
N(1)−C(2)	1.329(5)	C(2)−C(8)	1.484(5)
N(1)−C(10)	1.472(5)	C(3)−C(4)	1.378(6)
N(2)−N(3)	1.188(5)	C(4)−C(5)	1.370(6)
N(3)−N(4)	1.156(6)	C(5)−C(6)	1.379(6)
N(2′)−N(3′)	1.105(6)	C(6)−C(7)	1.385(6)
N(3′)−N(4′)	1.177(6)	C(7)−C(8)	1.408(5)
N(9)−C(8)	1.342(5)	C(10)−C(11)	1.515(6)
C(11)−C(12)	1.522(6)	C(20)−C(21)	1.390(6)
C(13)−C(14)	1.519(6)	C(21)−C(22)	1.380(6)
C(14)−C(15)	1.500(6)	C(22)−C(23)	1.409(5)
C(17)−C(18)	1.420(6)	C(25)−C(26)	1.496(6)
C(17)−C(23)	1.481(5)	C(26)−C(27)	1.521(6)
C(18)−C(19)	1.376(6)	C(28)−C(29)	1.515(5)
C(19)−C(20)	1.373(6)	C(29)−C(30)	1.527(5)

N(9)−Sn(1)−N(1)	73.0(1)	C(5)−C(4)−C(3)	130.3(4)
N(9)−Sn(1)−N(2)	94.5(1)	C(4)−C(5)−C(6)	126.0(4)
N(1)−Sn(1)−N(2)	87.9(1)	C(5)−C(6)−C(7)	129.9(4)
N(24)−Sn(2)−N(16)	73.7(1)	C(6)−C(7)−C(8)	132.7(4)
N(24)−Sn(2)−N(2′)	93.5(1)	N(9)−C(8)−C(7)	121.4(4)
N(16)−Sn(2)−N(2′)	93.7(1)	N(9)−C(8)−C(2)	114.3(3)
C(2)−N(1)−C(10)	119.5(3)	C(7)−C(8)−C(2)	124.3(4)
C(2)−N(1)−Sn(1)	118.8(2)	N(1)−C(10)−C(11)	112.2(3)
C(10)−N(1)−Sn(1)	121.7(2)	C(10)−C(11)−C(12)	110.9(4)
N(3)−N(2)−Sn(1)	117.5(3)	N(9)−C(13)−C(14)	113.1(3)
N(4)−N(3)−N(2)	177.3(4)	C(15)−C(14)−C(13)	112.3(4)
N(3′)−N(2′)−Sn(2)	119.1(3)	N(16)−C(17)−C(18)	121.2(3)
N(2′)−N(3′)−N(4′)	179.5(5)	N(16)−C(17)−C(23)	115.1(3)
C(8)−N(9)−C(13)	120.7(3)	C(18)−C(17)−C(23)	123.7(4)
C(8)−N(9)−Sn(1)	119.5(2)	C(19)−C(18)−C(17)	132.9(4)
C(13)−N(9)−Sn(1)	119.7(2)	C(20)−C(19)−C(18)	130.8(4)
C(17)−N(16)−C(25)	120.1(3)	C(19)−C(20)−C(21)	124.8(4)
C(17)−N(16)−Sn(2)	118.1(2)	C(22)−C(21)−C(20)	130.5(4)
C(25)−N(16)−Sn(2)	121.7(2)	C(21)−C(22)−C(23)	132.5(4)
C(23)−N(24)−C(28)	120.2(3)	N(24)−C(23)−C(22)	120.7(3)
C(23)−N(24)−Sn(2)	118.5(2)	N(24)−C(23)−C(17)	114.5(3)
C(28)−N(24)−Sn(2)	121.3(2)	C(22)−C(23)−C(17)	124.8(4)
N(1)−C(2)−C(3)	121.4(4)	N(16)−C(25)−C(26)	112.4(3)
N(1)−C(2)−C(8)	114.3(3)	C(25)−C(26)−C(27)	111.6(4)
C(3)−C(2)−C(8)	124.2(4)	N(24)−C(28)−C(29)	112.8(3)
C(4)−C(3)−C(2)	132.5(4)	C(28)−C(29)−C(30)	110.4(3)

calculation employed a basis set denoted **B2**, which consisted of the SBK basis set for all atoms[32] supplemented by diffuse and polarization functions on H and N ($\zeta_{D,H} = 0.036$, $\zeta_{D,N} = 0.0639$, $\zeta_{P,H} = 1.100$, and $\zeta_{P,N} = 0.800$). The metal polarization functions were the same as in **B1**. The CASSCF included 10 electrons and 12 orbitals, yielding 85590 configuration state functions in C_s symmetry. B3LYP calculations with the same basis set were also carried out on H−Ge−N_3 and H−Sn−N_3 for comparison.

Scheme 1

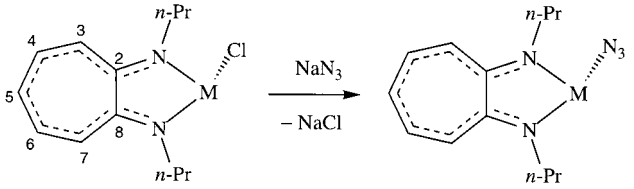

Results and Discussion

Interestingly, the reaction of $[(n\text{-Pr})_2\text{ATI}]GeCl$ or $[(n\text{-Pr})_2\text{ATI}]SnCl$ with NaN_3 in THF led to the corresponding azide $[(n\text{-Pr})_2\text{ATI}]GeN_3$ or $[(n\text{-Pr})_2\text{ATI}]SnN_3$ in excellent yield (Scheme 1). These Ge(II) and Sn(II) azides are dark yellow solids. Both $[(n\text{-Pr})_2\text{ATI}]GeN_3$ and $[(n\text{-Pr})_2\text{ATI}]SnN_3$ are soluble in polar solvents like CH_2Cl_2 or THF. The germanium azide $[(n\text{-Pr})_2\text{ATI}]GeN_3$ is also very soluble in toluene and moderately soluble in hexane. The tin analogue shows much less solubility in these hydrocarbon solvents (especially in hexane) perhaps indicating more ionic contribution to the structure. $[(n\text{-Pr})_2\text{ATI}]SnN_3$ shows better thermal and air stability compared to the germanium analogue. Upon heating, the germanium species $[(n\text{-Pr})_2\text{ATI}]GeN_3$ decomposes around 57 °C to a red liquid. The tin analogue melts at 93 °C without any apparent decomposition.

The germanium(II) and tin(II) azides were characterized by NMR and IR spectroscopy and by X-ray crystallography. ^{1}H NMR spectra of $[(n\text{-Pr})_2\text{ATI}]GeN_3$ and $[(n\text{-Pr})_2\text{ATI}]SnN_3$ show three well-defined sets of multiplets in the aromatic region, which can be assigned to H(5), H(3,7), and H(4,6), indicating the presence of a C_2 symmetric species in solution. ^{13}C NMR spectra show only four signals for ring carbon atoms C(2,8), C(4,6), C(3,7), and C(5), consistent with a fairly symmetric C_7N_2M (M = Ge or Sn) skeleton. IR spectra of $[(n\text{-Pr})_2\text{ATI}]GeN_3$ and $[(n\text{-Pr})_2\text{ATI}]SnN_3$ in KBr display a strong absorption band at 2048 and 2039 cm^{-1}, respectively. These bands can be assigned to the N_3 asymmetric stretching vibrations. The slightly higher $\nu_{asym}(N_3)$ value for the germanium analogue is consistent with the trend observed for germanium(IV) and tin azides(IV) (e.g., Me_3GeN_3, 2103 cm^{-1}; Me_3SnN_3, 2045 cm^{-1})[5] and is consistent with the theoretical calculations on the corresponding *N*-methyl-substituted species $[(Me)_2\text{ATI}]MN_3$, which predict ν_{asym} values of 2049 and 2048 cm^{-1} for the germanium and tin systems, respectively (Table 4). The $\nu_{asym}(N_3)$ value of $[(n\text{-Pr})_2\text{ATI}]GeN_3$ is similar to that observed for the tris(pyrazolyl)-boratogermanium(II) adduct $[HB(3,5\text{-}(CH_3)_2Pz)_3]GeN_3$ (ν_{asym}-

(27) Frisch, M. J.; Trucks, G. W.; Schlegel, H. B.; Scuseria, G. E.; Robb, M. A.; Cheeseman, J. R.; Zakrzewski, V. G.; Montgomery, J. A., Jr.; Stratmann, R. E.; Burant, J. C.; Dapprich, S.; Millam, J. M.; Daniels, A. D.; Kudin, K. N.; Strain, M. C.; Farkas, O.; Tomasi, J.; Barone, V.; Cossi, M.; Cammi, R.; Mennucci, B.; Pomelli, C.; Adamo, C.; Clifford, S.; Ochterski, J.; Petersson, G. A.; Ayala, P. Y.; Cui, Q.; Morokuma, K.; Malick, D. K.; Rabuck, A. D.; Raghavachari, K.; Foresman, J. B.; Cioslowski, J.; Ortiz, J. V.; Stefanov, B. B.; Liu, G.; Liashenko, A.; Piskorz, P.; Komaromi, I.; Gomperts, R.; Martin, R. L.; Fox, D. J.; Keith, T.; Al-Laham, M. A.; Peng, C. Y.; Nanayakkara, A.; Gonzalez, C.; Challacombe, M.; Gill, P. M. W.; Johnson, B. G.; Chen, W.; Wong, M. W.; Andres, J. L.; Head-Gordon, M.; Replogle, E. S.; Pople, J. A. *Gaussian 98*, revision A.7; Gaussian, Inc.: Pittsburgh, PA, 1998.

(28) Becke, A. D *Phys. Rev. A* **1988**, **38**, 3098. Lee, C.; Yang, W.; Parr, R. G. *Phys. Rev. B*, **1988**, *37*, 785. Becke, A. D. *J. Chem. Phys.* **1992**, *96*, 2155.

(29) Andrae, D.; Haussermann, U.; Dolg, M.; Stoll, H.; Preuss, H. *Theor. Chim. Acta* **1990**, *77*, 123. Obtained from the Extensible Computational Chemistry Environment Basis Set Database, Version 1.0, as developed and distributed by the Molecular Science Computing Facility, Environmental and Molecular Sciences Laboratory, which is part of the Pacific Northwest Laboratory, P.O. Box 999, Richland, WA 99352, USA, and funded by the U.S. Department of Energy. The Pacific Northwest Laboratory is a multiprogram laboratory operated by Battelle Memorial Institute for the U.S. Department of Energy under Contract DE-AC06-76RLO 1830. Contact David Feller, Karen Schuchardt, or Don Jones for further information.

(30) Reed, A. E.; Curtiss, L. A.; Weinhold, F. *Chem. Rev.* **1988**, *88*, 899 and references therein.

(31) Schmidt, M. W.; Baldridge, K. K.; Boatz, J. A.; Elbert, S. T.; Gordon, M. S.; Jensen, J. J.; Koseki, S.; Matsunaga, N.; Nguyen, K. A.; Su, S.; Windus, T. L.; Dupuis, M.; Montgomery, J. A *J. Comput. Chem.* **1993**, *14*, 1347.

(32) Stevens W. J.; Basch, M.; Krauss, M. *J. Chem. Phys.* **1984**, *81*, 6026. Stevens W. J.; Basch, M.; Krauss, M.; Jasien, P.; *Can. J. Chem.* **1992**, *70*, 612. Cundari, T. R.; Stevens, W. J. *J. Chem. Phys.* **1993**, *98*, 5555.

Table 4. Calculated N−N Stretching Frequencies for $[(Me)_2ATI]MN_3$

	calcd[a]		exptl	
M	as	ss	as	ss
Ge	2049	1253	2048	
Sn	2048	1260	2039	

[a] In cm^{-1}, scaled by 0.94; as = asymmetric stretch; ss = symmetric stretch. Experimental values from $[(n\text{-}Pr)_2ATI]MN_3$ analogues.

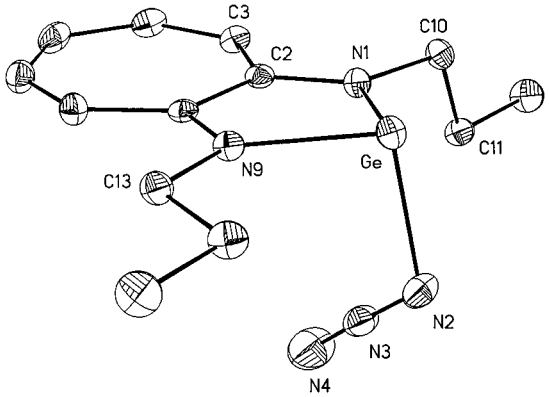

Figure 1. Molecular structure of $[(n\text{-}Pr)_2ATI]GeN_3$. Hydrogen atoms have been omitted for clarity.

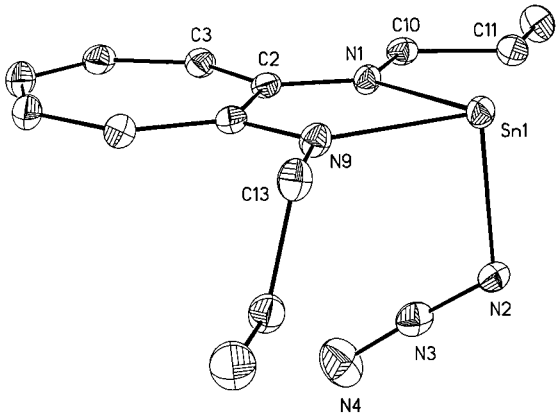

Figure 2. Molecular structure of $[(n\text{-}Pr)_2ATI]SnN_3$. Only one of the two in the asymmetric unit is shown, and hydrogen atoms have been omitted for clarity.

(N_3) = 2043 cm^{-1}).[17] Ionic azides such as $[N(CH_3)_4]N_3$ show the corresponding $\nu_{asym}(N_3)$ at a lower frequency (1998 cm^{-1}).[33] Unfortunately, we could not assign unambiguously the $\nu_{sym}(N_3)$ IR bands for $[(n\text{-}Pr)_2ATI]GeN_3$ and $[(n\text{-}Pr)_2ATI]SnN_3$ (generally expected in the region 1350−1250 cm^{-1}) due to interference from other ligand-based absorption bands. The theoretical predictions for these bands for the related $[(Me)_2ATI]MN_3$ systems are 1253 cm^{-1} (M = Ge) and 1260 cm^{-1} (M = Sn) (Table 4).

The X-ray crystal structures of $[(n\text{-}Pr)_2ATI]GeN_3$ and $[(n\text{-}Pr)_2ATI]SnN_3$ are shown in Figures 1 and 2, respectively. $[(n\text{-}Pr)_2ATI]GeN_3$ shows a monomeric structure (closest intermolecular Ge···Ge and Ge···N separations are 3.73 and 4.43 Å, respectively). The asymmetric unit of $[(n\text{-}Pr)_2ATI]SnN_3$ contains two chemically similar, but crystallographically different, molecules. One of these (containing Sn1) exhibits weak intermolecular Sn···N(azide) contacts at 2.87 Å. $[(n\text{-}Pr)_2ATI]GeN_3$ and $[(n\text{-}Pr)_2ATI]SnN_3$ have pyramidal Ge and Sn sites.

(33) Christe, K. O.; Wilson, W. W.; Bau, R.; Bunte, S. W. *J. Am. Chem. Soc.* **1992**, *114*, 3411−3414.

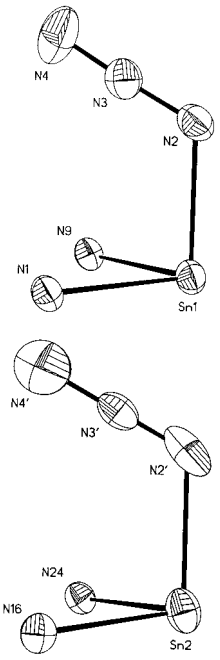

Figure 3. Two molecules of $[(n\text{-}Pr)_2ATI]SnN_3$ in the asymmetric unit. Only tin and nitrogen atoms are shown.

Heterobicyclic C_7N_2Ge and C_7N_2Sn moieties are essentially planar. Azide groups occupy a site above the ring systems (cis), although there is no obvious reason that the trans arrangement should be less stable. Indeed, DFT calculations indicate that the trans arrangements are only very slightly less stable, 0.2 and 0.5 kcal/mol for the germanium and tin species, respectively. The Ge−N(azide) and Sn−N(azide) distances are 2.047(2) and 2.241(4) Å, respectively. A longer distance for the tin analogue is expected on the basis of the larger atomic radius of Sn. The Ge−N(azide) bond distance of $[(n\text{-}Pr)_2ATI]GeN_3$ is significantly shorter than that of $[HB(3,5\text{-}(CH_3)_2Pz)_3]GeN_3$ (2.262(4) Å). This may be due to the smaller coordination number at germanium (3 rather than 4) in $[(n\text{-}Pr)_2ATI]GeN_3$.

The azide groups of $[(n\text{-}Pr)_2ATI]GeN_3$ and $[(n\text{-}Pr)_2ATI]SnN_3$ are almost linear as is evident from the N−N−N bond angles of 177.5(3)° and 178.4(4)°, respectively. The N−N bond distances of $[(n\text{-}Pr)_2ATI]GeN_3$ are 1.197(3) and 1.144(4) Å. These values may be compared to the corresponding N−N bond distances of 1.136(5) and 1.179(6) Å in $[HB(3,5\text{-}(CH_3)_2Pz)_3]GeN_3$. Two $[(n\text{-}Pr)_2ATI]SnN_3$ molecules in the asymmetric unit exhibit different N−N bond lengths. Although molecular packing forces etc. can have an effect on some of these structural data, this difference in observed N−N distances may be most likely a result of minor disorder (particularly along the NNN axis in the Sn2 molecule) as is evident from the thermal ellipsoid plots of the azide moiety (Figure 3). The N−N distances of the molecule containing Sn1 are very similar to those of the germanium analogue $[(n\text{-}Pr)_2ATI]GeN_3$. The solid state and solution IR data and the calculated stretching frequency values are also consistent with similar azide moieties in $[(n\text{-}Pr)_2ATI]GeN_3$ and $[(n\text{-}Pr)_2ATI]SnN_3$. However, if we were to consider the average (Sn)N−N and (N)N−N distances of both molecules (1.146 and 1.167 Å, respectively), they are much closer to those observed for the tris(pyrazolyl)boratogermanium species. There is some ionic contribution to the Ge−N_3 bonding in $[HB(3,5\text{-}(CH_3)_2Pz)_3]GeN_3$. For comparison, ionic azides such as $[N(CH_3)_4]N_3$ have linear N_3 units with equal N−N distances (1.16 Å).[4,33]

The bonding in MN_3 species may be described by two main canonical forms: M−N=N=N and M−N−N≡N (where M =

Table 5. Optimized Geometrical Parameters and Their Experimental Counterparts[a]

	$N_{ring}-Ge$	Ge−N(2)	N(2)−N(3)	N(3)−N(4)	Ge−N(2)−N(3)	N(2)−N(3)-N(4)
			$[(Me)_2\text{ATI}]GeN_3$			
calcd	2.024	2.049	1.221	1.153	117.1	178.5
exptl	1.951	2.047	1.197	1.144	115.3	177.5
			$[(Me)_2\text{ATI}]SnN_3$			
	$N_{ring}-Sn$	Sn−N(2)	N(2)−N(3)	N(3)−N(4)	Sn−N(2)−N(3)	N(2)−N(3)-N(4)
calcd	2.210	2.217	1.220	1.154	118.3	178
exptl	2.156−2.190	2.230, 2.253	1.105, 1.188	1.156, 1.177	117.5, 119.1	177.3, 179.5

[a] Å and deg, experimental values from $[(n\text{-Pr})_2\text{ATI}]MN_3$ analogues.

Table 6. Natural Bond Orbital Analysis for $[(Me)_2\text{ATI}]GeN_3$ and $[(Me)_2\text{ATI}]SnN_3$

occupancies	Lewis structure	atoms
Ge		
1.667	bond	Ge−N(2)
1.956	lone pair	Ge
1.996	bond	N(2)−N(3)
1.996	bond	N(3)−N(4)
1.992	bond	N(3)−N(4)
1.985	bond	N(3)−N(4)
Sn		
1.633	bond	Sn−N(2)
1.967	lone pair	Sn
1.996	bond	N(2)−N(3)
1.996	bond	N(3)−N(4)
1.991	bond	N(3)−N(4)
1.986	bond	N(3)−N(4)

Table 7. NBO Charges for $[(Me)_2\text{ATI}]MN_3$

	ring	M	N(2)	N(3)	N(4)	azide
M = Ge	−0.495	1.169	−0.208	0.207	−0.673	−0.674
M = Sn	−0.606	1.291	−0.219	0.233	−0.699	−0.685

Ge or Sn). In addition, an ionic resonance form $M^+[N_3]^-$ may also contribute to a certain degree to the overall bonding picture. Thus, in order to better understand the bonding between an azide moiety and germanium(II) or tin(II), we performed a detailed computational study on the very closely related $[(Me)_2\text{ATI}]MN_3$ (where M = Ge or Sn). The relevant optimized geometrical parameters and their experimental counterparts are presented in Table 5. In general, the calculated M−N and N−N distances agree well with experiment, although comparisons with the Sn system are difficult because of the significant structural differences in the azide moiety of the two crystallographically different molecules in the unit cell. The DFT results are, however, unambiguous. The calculated N−N bond lengths in both germanium and tin systems are essentially identical and strongly suggest that the dominant canonical form of the metal−azide moiety is M−N−N≡N. The calculated N−N stretching frequencies (Table 4) and a natural bond orbital (NBO) analysis (Table 6) lead to the same conclusions. In particular, the NBO analyses of the two species are nearly identical, with one strongly occupied N(2)−N(3) and three strongly occupied N(3)−N(4) natural orbitals (where N(2) is the nitrogen atom bonded to Ge or Sn). The natural charges (Table 7) are also nearly identical for the azide nitrogens, although significant differences in the charges of the metals and the $[(Me)_2\text{ATI}]$ ligand exist. As expected on the basis of electronegativity arguments, the Sn system exhibits a more positive metal and more negative ligands, although almost all (about 90%) of the excess negative charge on the ligands in the Sn system is found on the $[(Me)_2\text{ATI}]$ ring. This is hardly surprising, given the large size and highly delocalized nature of this ligand.

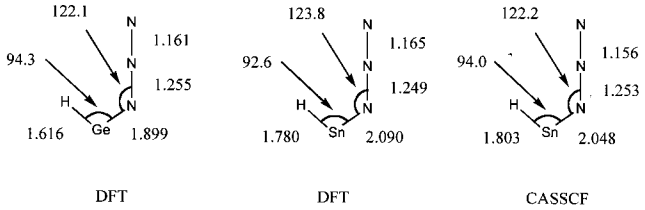

Figure 4. Comparison of the optimized geometries (Å and deg) of H−Ge−N_3 and H−Sn−N_3 at the DFT (B3LYP) level and H−Sn−N_3 at the CASSCF.

One potential area of concern in the DFT calculations is the accuracy of the DFT approach for species which, because of the presence of the azide ligand and an adjacent carbene type lone pair on the main group element, almost certainly have a manifold of low-lying excited states and may well require a multiconfiguration wave function for a reasonable description of the ground state. To probe this issue, we performed a CASSCF geometry optimization on H−Sn−N_3 using the **B2** basis set as described earlier. The resultant geometry, along with the corresponding geometries obtained at the B3LYP level with the same basis set for H−Ge−N_3 and H−Sn−N_3, is illustrated in Figure 4. Clearly, there are no significant differences in the N−N distances, strongly suggesting that the DFT results are reliable for the larger system discussed above. It is also clear from Figure 4 that even this simple model is consistent with the dominant resonance form M−N−N≡N for both germanium and tin.

In summary, this work shows that germanium(II) and tin(II) azide derivatives of aminotroponiminates can be isolated as thermally stable solids. $[(n\text{-Pr})_2\text{ATI}]GeN_3$ and $[(n\text{-Pr})_2\text{ATI}]SnN_3$ represent a very rare group of azides that feature low valent group 14 elements. We are currently exploring the chemistry of other relatives of this family.

Acknowledgment. We thank The Robert A. Welch Foundation (Grants Y-1289 to H.V.R.D. and Y-0743 to D.S.M.) for support of this work. We also thank the National Science Foundation (CHE-9601771) for providing funds to purchase the 500 MHz NMR spectrometer.

Supporting Information Available: X-ray crystallographic files in the CIF format and optimized Cartesian coordinates for $[(Me)_2\text{ATI}]GeN_3$ and $[(Me)_2\text{ATI}]SnN_3$. This material is available free of charge via the Internet at http://pubs.acs.org.

IC000545U